Article

$Ce_{0.8-2x}Sm_{0.2}Zr_xMg_xO_{2-d}$, {x= 0.05, 0.1 &0.15} Promising electrolyte Compounds with remarkable conductivities for Intermediate Solid Oxide Fuel Cells (IT-SOFCs) Applications

Abdalla.M Abdalla [1,2,*], Abul K Azad [3], Mohamed M k Dawood [1] and Juantakan Taweekun [2,*]

[1] Mechanical Engineering Department, Faculty of Engineering, Suez Canal University, Ismailia 41522, Egypt
[2] Department of Mechanical and Mechatronics Engineering, Faculty of Engineering, Prince of Songkla University, Hatyai 90112, Songkhla, Thailand
[3] Faculty of Integrated Technologies, Universiti Brunei Darussalam, Jalan Tungku Link, Gadong BE 1410, Brunei Darussalam
* Correspondence: juntakan.t@psu.ac.th (J.T.); abdalla.m.abdalla@eng.suez.edu.eg (A.M.A.)

Abstract: CSZM compounds were synthesized by dry chemistry route with 5, 10, and 15% dopant of Mg dopants in the $Ce_{0.8-2x}Sm_{0.2}Zr_xMg_xO_{2-d}$, {x = 0.05, 0.1 &0.15}. The newly investigated materials were physically, chemically, and electrochemically studied and have shown promising results. The CSZM was crystalized in a fluorite structure with a pure cubic phase in a space group Fm3m and cell parameter a = 5.401742 $°A$ and theoretical density from 7.6 to 8.9 after firing in the air with a final temperature of 1400 °C. characterization of the structure and indexing of electrolyte materials were made after X-ray diffraction (XRD) testing. A Scanning electron microscope (SEM) morphological analysis was used to examine the microstructure details. Electronic impedance spectroscopy (EIS) measurements were achieved from 400 °C to 700 °C showing the highest value of conductivity of 1.0461 x 10^{+1} S/cm at 700 °C while the minimum value was 2.7329 x 10^{-2} S/cm at 400 °C and the total activation energy was found (E_a) 0.6865 eV under 5% H_2/Ar.

Keywords: solid oxide fuel cells; biomass; electrolyte; conductivity

1. Introduction

The shift from dependence on fossil fuels to renewable energy resources is very necessary nowadays, especially with their zero-pollution impacts like in solar cells, fuel cells, and other types of renewables [1–5]. Solid oxide fuel cell (SOFC) devices recently proved their highly remarkable source of chemical clean energy conversions. The main structure of these devices is defined by two electrodes (Anode and Cathode) detached by highly dense electrolyte materials generating power through electrochemical reactions [1,2]. The used electrolyte can be a proton ion conductor, otherwise an oxygen ion conductor [2–4], and they should be relatively or closely compacted, durable, and chemically and thermally stable in a reducing and oxidizing environment [5–7].

The more important thing recently investigated is using an integrated system from biomass gasification and fuel cells together [8–14] to get higher performance and supply more power. And after developing new materials to be applied in SOFCs, there is a higher potential to apply it in biomass-gasification fuel cell systems investigated in many research works [8]. Since H_2 exists as a low-density gas, posing a significant storage challenge. Hydrogen storage in the case of solid state and liquid methods relying on metal hydrides outperforms traditional bulky gaseous in terms of protection, production costs, and density [15–17]. MgH_2 is one of the most effective types among light hydrides with reversible H_2 storage due to its capacity for high hydrogen storage, its reversibility, and H_2 storage abundance reserves on Earth [18–20].

 doi:10.20944/preprints202306.0496.v1

In the last two decades, scientists and researchers were seeking high-performance techniques to investigate material properties and they were focusing on Magnesium based hydrogen [15,21] with remarkable activities, especially with doping of Mg-oxides [22]. The addition of metal oxides (Fe_2O_3, Nb_2O_5, CeO_2, etc.) [16,23,24] or (Ni, Co, Fe, etc.) transition metals [15,25,26] to magnesium were reported as an effective candidate due to their altered reaction pathway in optimized thermodynamics [27]. Hence, developing new electrolyte materials through rare earth elements in single or multi-dopants is essentially required when applied in SOFC devices. Thereby, Lanthanides doped cerium { Sm, Gd, Nd } based materials have shown preferred closely or relatively compacted electrolytes applied in SOFCs at intermediate or low-temperature levels (IT/LT- SOFCs) [28–34]. These based crystalline structures are dry and wet chemical synthesized and have introduced high oxygen ionic conductivities at temperature ranges from 500 to 800 °C [35,36]. The single or multi-dopant ceria-based Rare-earth and alkaline- elements have greatly enhanced the ionic conductivities at a reduced temperature range compared with common electrolyte ones YSZ [37–39]. But introducing Mg doped in these compounds will be expected to show remarkable results in obtained power and the whole performance of the designed system. Many trials were made to investigate the use of Mg in various applications through energy devices as introduced by V.A. Yartys et al. [40] and recent work done through fuel cell devices. A trial was made by Jianjiang Hu et al., [41] where a high-temperature PEM fuel cell stack was used for a prototype auxiliary power unit, through the application of Li-Mg-N-H, they succeeded to get the Max working temperature being 200 °C with a designed output of 1 kW. While, Jingfeng Xue et al., [42] used pure perovskite Mg co-doped compounds at intermediate temperature SOFCs. They have got power of 0.5 Wcm^{-2} at 600 °C and max power of 0.8 Wcm^{-2} at 850 °C.

Flores et al [43] have made recently an investigation of a multi-dopant including Mg co-doped compound as double perovskites derived material Sr_2MgMoO_{6-d} as anode with potential application in SOFCs and succeeded to introduce materials able to show acceptable electrical conductivity, power density, and thermal expansion coefficient, in redox environments synthesized through various techniques.

In the current study, $Ce_{0.8-2x}Sm_{0.2}Zr_xMg_xO_{2-d}$ series of materials were synthesized {x = 0.05, 0.1 &0.15} as novel electrolyte compounds working in both intermediate and high-temperature ranges applied in SOFC devices which can be also used in an integrated system of biomass gasification with SOFC. Mg doping has shown a very significant and good impact on hydrogen storage capacity and as a result, we are trying to confirm this investigation by doping it in some materials that can be applied in fuel cell applications. The obtained results have shown the potential of applying Mg as electrolyte materials and it can also be used in electrode materials as well in SOFCs devices. Physical and electrochemical characterization for the materials were made and the obtained results showed remarkable results in both physical characterizations and the output power.

2. Experimental

2.1. CSZM materials synthesis

Series of Mg_x doped $Ce_{0.8-2x}Sm_{0.2}Zr_xO_{2-d}$, {x= 0.05, 0.1 &0.15} were synthesized using solid-state chemistry method in the air at 1400 °C for 12 hours inside a muffle furnace. The chemicals of CeO_2, ZrO_2, Sm_2O_3, and MgO in precise stoichiometric ratios were used from Sigma Aldrich (purity of more than 99.95%). Collected powders were preheated at 350 °C for 8 hours in a muffle furnace for humidity and re-carbonation avoidance followed by quick weight on an accurate digital microbalance. All compounds with a little amount of acetone CH_3COCH_3 were hand mixed in an agate mortar pestle for almost 2 hours. The ball milling technique was followed in the previous step to get a homogenous mixture of the compounds with an appropriate amount of ethanol C_2H_5OH for 48 hours. Afterward, a mixture of ball-milled compounds was collected and dried in a fume hood overnight. Finally, the collected powders were heated on a magnetic hotplate at 70 °C for 4 hours of each composition. The calcination process at 800 °C for 12 hours was achieved for the collected powders at a rate of 5 °C/min (heating and cooling). Again, samples were ground for 45 Minutes with

Preprints (www.preprints.org) | NOT PEER-REVIEWED | Posted: 7 June 2023 doi:10.20944/preprints202306.0496.v1

a small amount of binder of terpineol before being compressed to form pellets of 2 grams 20 mm in diameter using the hydraulic press of 100 MPa. The formed pellets were fired at 1200 °C in the air for 12 hours in a carbolite furnace. Following that the X-Ray diffraction (XRD) for the compounds was checked to confirm the phase purity and reaction. Then again after regrinding like the earlier stage, CSZM pellets again sintered at a final temperature of 1400 °C for 12 hours to achieve a single phase and complete reaction of all synthesized series. Figure 1 summarizes the preparation process until getting the final pure phase.

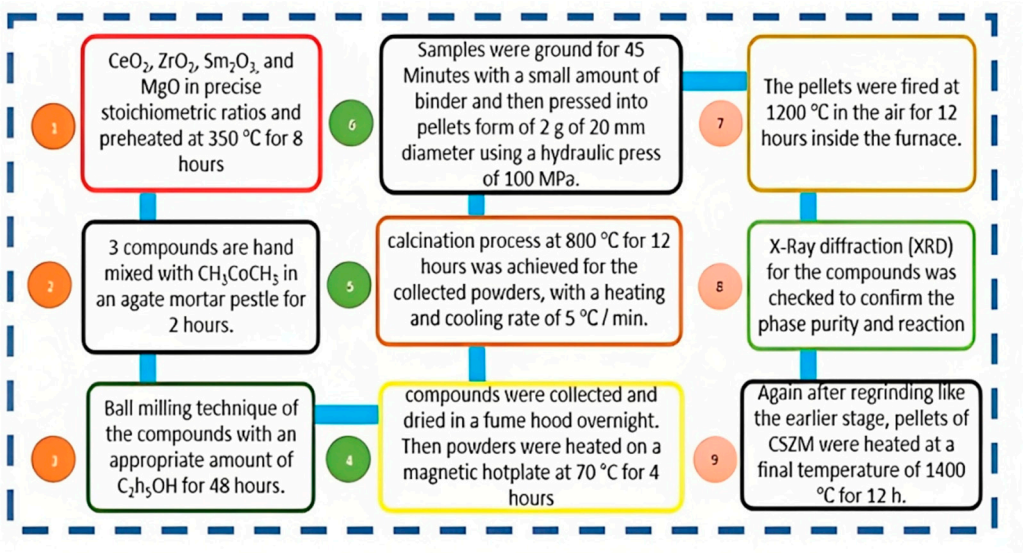

Figure 1. Summary of the preparation process using solid-state reaction method to get confirmed structure of CSZM in a single structure pure phase.

2.2. Characterizations of the samples

The thermal response and behavior of the formed materials were investigated for the uncalcined powder through thermogravimetric analysis (TGA) PerkinElmer, STA 6000, USA in a range of 50 to 1000 °C and rate of 5 °C/min with flowing nitrogen 50 ml/min where samples were kept isothermally for 30 min at the final temperature. After that, the XRD patterns of the synthesized samples for Mg_x doped $Ce_{0.8-2x}Sm_{0.2}Zr_xO_{2-d}$, {x= 0.05, 0.1 &0.15} where D8 Advanced Bruker XRD system with CuKα1 radiation of λ = 1.5406 Å and using 2θ = 10° to 90° angular range with 0.02° step size in RT. After XRD data were collected then WinXpow and TREOR90 [44] were used for indexing. Following the previous step, Rietveld refinements analysis of XRD data was done carefully using the FullProf suite [45]. Scanning electron microscope (SEM) of JEOL 5600 was used for studying the microstructure and crystal features for the 3 synthesized compounds of 5%,10%, and 15%. In addition investigation of Energy-dispersive X-ray Spectroscopy (EDX) analysis for the tested samples for element percentage in the final formed compound. For impedance measurements and analysis, a Solartron EIS spectrometer that has a frequency response analyzer was utilized. Where, a symmetrical cell was prepared to have a size of 13 mm Diameter ~1.1 mm thickness, where on both sides of the tested pellet platinum paste was printed with an effective area of 1cm^2. Afterward, the tested pellet was inserted in the furnace for drying at 700 °C for 1 h. In the impedance measurement, stage 50 mA current amplitude was applied in a range of temperature 300 to 800 °C with a stepped temperature of 50 °C and of 3 °C /min heating rate in a wet 5 %H_2/Ar with a range of frequency from1 MHz to 10 MHz.

3. Results and discussion

3.1. Structural and phase analysis of XRD data

Preprints (www.preprints.org) | NOT PEER-REVIEWED | Posted: 7 June 2023 doi:10.20944/preprints202306.0496.v1

The collected data of XRD spectra for the 3 synthesized series of Mg_x doped $Ce_{0.8-2x}Sm_{0.2}Zr_xO_{2-d}$, x= 0.05, 0.1 &0.15} were analyzed by Rietveld analysis at RT after the final sintering temperature of 1400 °C is appearing in Figure 2 below with peak indexing showing the single-phase purity. The Rietveld analyses of the XRD patterns of all materials confirm a stable single-phase cubic structure in the F m-3m fluorite type in a space group with nearly similar cell parameter a= 5.4 ^{0}A for all compounds.

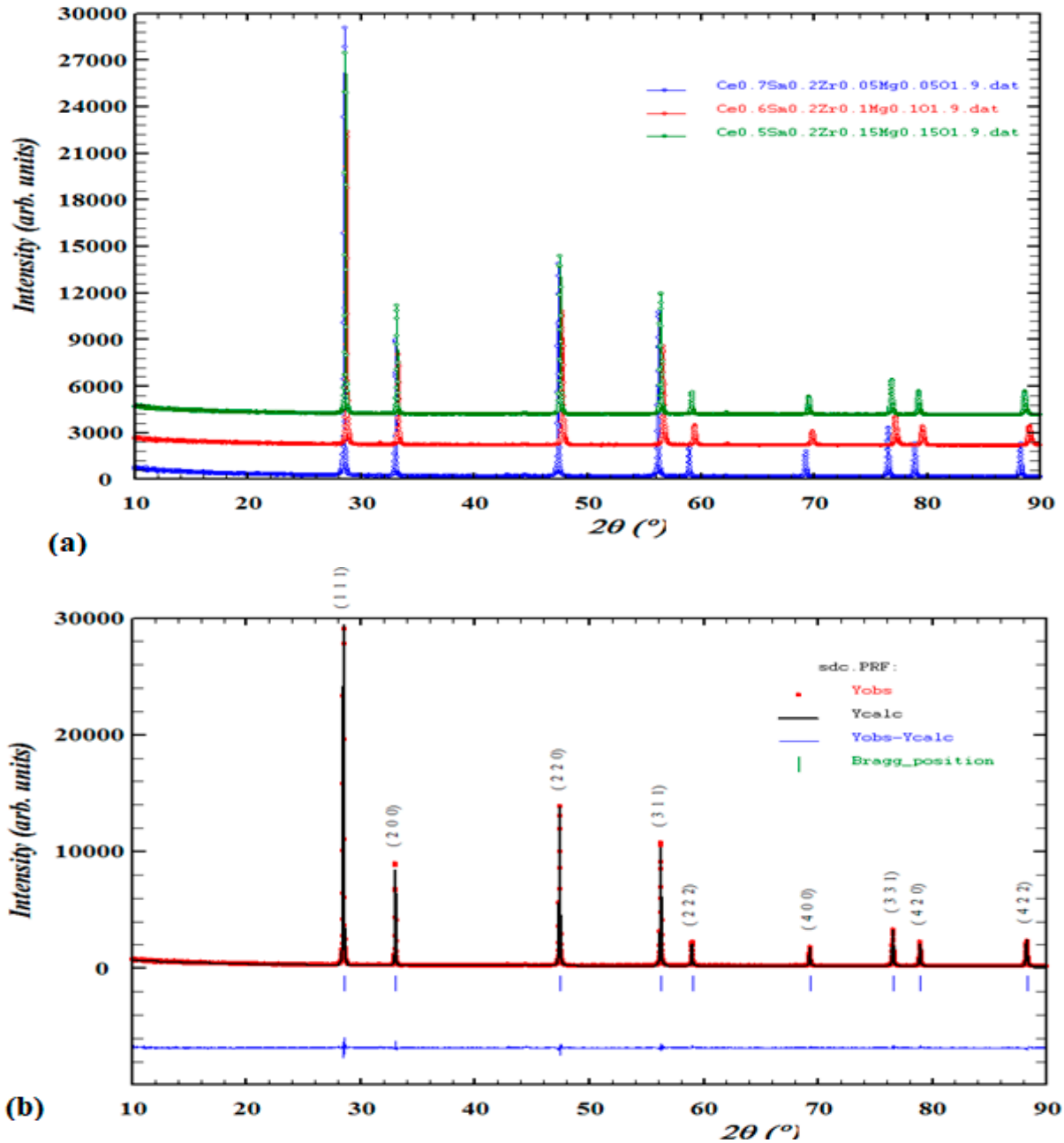

Figure 2. a) XRD patterns of $Ce_{0.7}Sm_{0.2}Zr_xMg_xO_{1.9}$, $Ce_{0.6}Sm_{0.2}Zr_xMg_xO_{1.9}$, $Ce_{0.5}Sm_{0.2}Zr_xMg_xO_{1.9}$ x={0.05, 0.1, 0.15} and b) Rietveld refinement analysis of a single pure phase material with indexed peaks.

Due to the indexed peaks with Winx POW and TREOR90 software the existence of sharp peaks like in (111), (200), (220) and (311) is because of well crystalline after the calcination process. Considering that values of observed minus calculated (obs-calc) represents indexed materials in a precise symmetry (cubic) and space group (F m-3m). following that the refinement parameters of all compounds are similar in their lattice in addition to the calculated theoretical density is almost very close in values when calculated using the following equation [46]:

Preprints (www.preprints.org) | NOT PEER-REVIEWED | Posted: 7 June 2023 doi:10.20944/preprints202306.0496.v1

$$\rho_{Th} = \frac{4\,M\,W_{CSZM}}{N_A\,a^3} \quad (1)$$

Where MW_{CSZM} is the molecular weight of CSZM electrolytes and NA is Avogadro's number, a representing lattice parameter as listed in Table 1 below. Rietveld refinement parameters of the CSZM materials showing similar values of lattice parameters as the samarium (Sm) amount is the same in the whole synthesized compounds and due to its ionic radius (0.958 Å, coordination number (CN) = 6) compared to cerium (Ce) (0.87 Å with the same CN) however density increased with increasing Mg doped amount from 5% to 15% due to the lattice parameter increase which directly affects the volume of the synthesized sample. The confirmed structure of the synthesized material after getting XRD patterns is obeying Vegard's law. It is clear also that the change that happened in the peak shift as shown in Fig 1a was due to the small change of lattice parameters and due to the increase of Mg % dopant results in an increase of tensile strength that mamakes this small shift of the plane towards the lower angle. And this also can be clearly observed from the lattice parameters and volume of the indexed XRD patterns from the given data in Table 1 and confirms this with previous work in the literature [47].

However, the atomic position of the multi-dopant is almost the same in the 3 compounds and that was due to the stability of the structure with higher densification of Mg doping and when the percentage increased from 5% to 15% porosity increased with grain growth increase at higher sintering temperature of 1400 °C.

Table 1. Synthesized series of CSZM in 5%, 10%, and 15% showing cell, refinement parameters theoretical densities value and atomic positions.

Chemical Compounds	Space group	a =b = c	Volume	X^2	R_p	R_{wp}	R_{exp}	Theoretical density
$Ce_{0.7}Sm_{0.2}Zr_{0.05}Mg_{0.05}O_{1.9}$	F m-3m	5.401742	159.1092	1.63	5.16	6.79	5.32	7.623
$Ce_{0.6}Sm_{0.2}Zr_{0.1}Mg_{0.1}O_{1.9}$	F m-3m	5.390912	155.80007	2.13	5.88	7.75	5.31	8.319
$Ce_{0.5}Sm_{0.2}Zr_{0.15}Mg_{0.15}O_{1.9}$	F m-3m	5.401577	157.5144	2.34	6.36	8.37	5.47	8.908

Atomic positions						
	$Ce_{0.7}Sm_{0.2}Zr_{0.05}Mg_{0.05}O_{1.9}$ (x , y, z) & $Ce_{0.6}Sm_{0.2}Zr_{0.1}Mg_{0.1}O_{1.9}$ (x , y, z)				$Ce_{0.5}Sm_{0.2}Zr_{0.15}Mg_{0.15}O_{1.9}$ (x , y, z)	
	Occ					
Ce	(0, 0 0)	0.7	(0, 0 0)	0.6	(0, 0 0)	0.5
Sm	(0, 0 0)	0.2	(0, 0 0)	0.2	(0, 0 0)	0.2
Zr	(0, 0 0)	0.05	(0, 0 0)	0.1	(0, 0 0)	0.15
Mg	(0, 0 0)	0.05	(0, 0 0)	0.1	(0, 0 0)	0.15
O	(0.25,0.25,0.25)	1.9	(0.25,0.25,0.25)	1.9	(0.25,0.25,0.25)	1.9

- **Surface morphology of synthesized samples using SEM & EDX**

Surface morphology and microstructure of the 3 synthesized compounds of electrolyte materials were carefully checked through SEM to show the level of densification at the 5%,10%, and 15% levels. Figure 3 shows clear view of the microstructures for CSZM compounds and images are showing that with higher doping of Mg resulted in higher porosity however, the final sintering temperature was 1400 °C. Thereby, the Mg doping has shown abnormal grain growth due to the thermomechanical treatments that have adirect effect and significant role in the investigation of the synthesized samples owing to the close dependence of properties upon grain size [48].

But the grain growth clearly occurred on 5% doping of Mg during the densification [49] compared to other percentages. 1 μm average grain size for the pellet sintered at 1200 °C, whereas for 1300 1.6 to 2.3 μm and at the final temperature of 1400 °C, the grain size ranged from 2.5 to 3.7 μm, From Figure 3a,c of the compound $Ce_{0.7}Sm_{0.2}Zr_{0.05}Mg_{0.05}O_{1.9}$. showing some inhomogeneity in grain sizes due to higher sintering temperatures, but the most interesting is getting well compact and dense electrolyte materials compared to the other 2 compounds. Some pores started to occur and with Mg doping increase, abnormal grain growth resulted in some pores being trapped inside the microstructure even with higher sintering temperatures it is difficult to erase [50–52]. The EDX

Preprints (www.preprints.org) | NOT PEER-REVIEWED | Posted: 7 June 2023 doi:10.20944/preprints202306.0496.v1

elemental analysis of CSZM was investigated as shown in Figure 4 and it shows from the selected spectrum the existence of all chemicals Ce, Sm, Zr, and Mg with a total percentage of 100% without any other impurities and proof of a full and complete solid-state reaction occurred for all compound showing a pure phase fluorite type. What was interesting, is the homogeneity of the surface and there is no existence of any impurities or agglomerations [52] and it is clearly observed in the selected spectrum, considering this case for all synthesized compounds with the different doping percentages of Mg 5%, 10% and 15%.

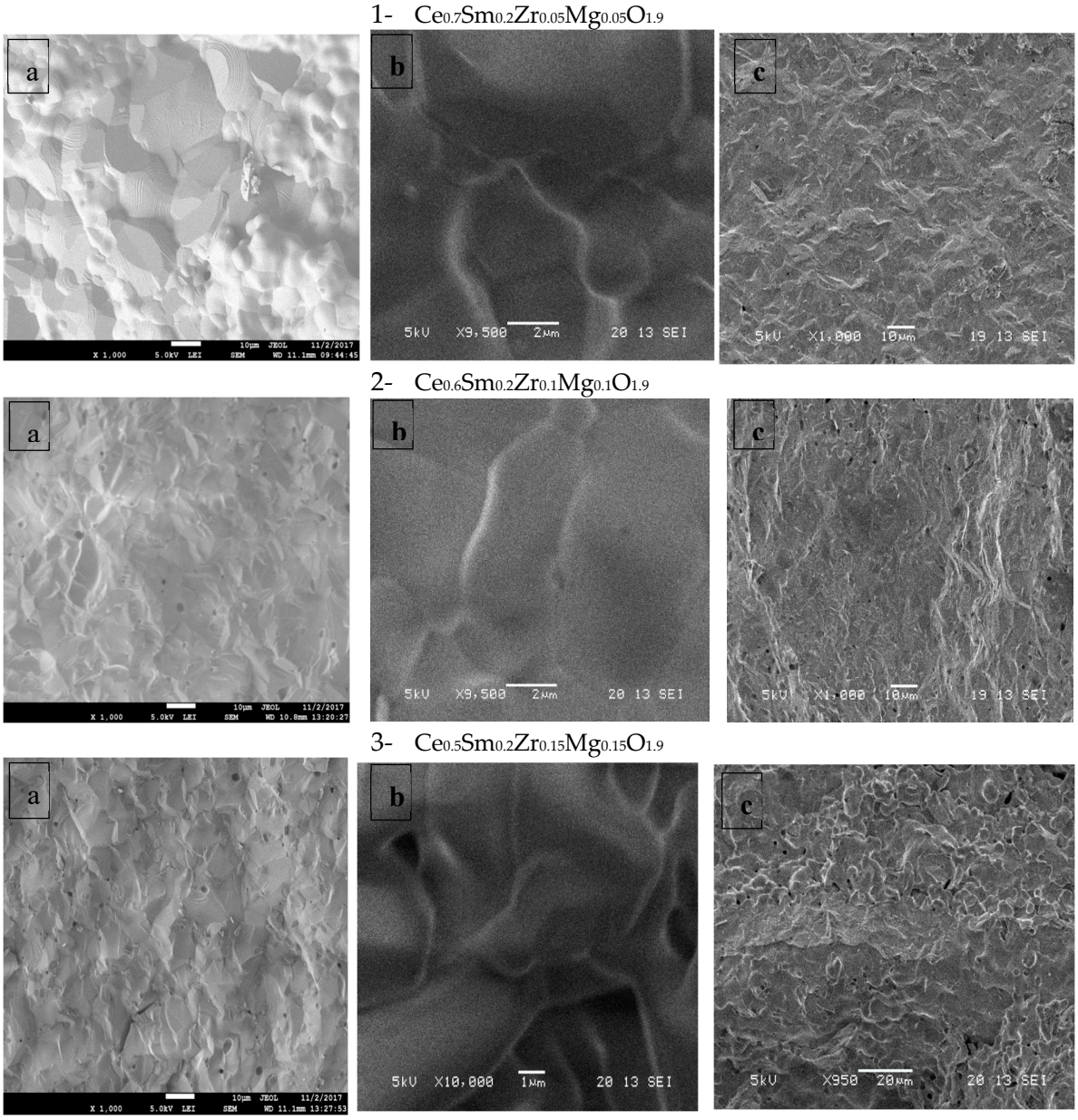

Figure 3. SEM images of a), b) surface, and c) Cross section for CSZM compounds in 5%,10%, and 15% doping.

Preprints (www.preprints.org) | NOT PEER-REVIEWED | Posted: 7 June 2023 doi:10.20944/preprints202306.0496.v1

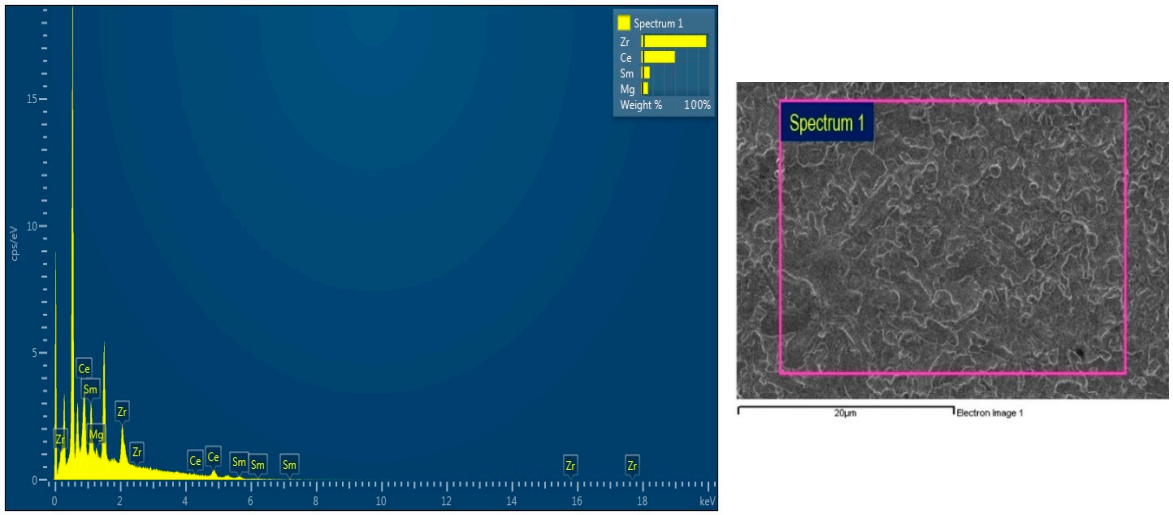

Figure 4. EDX analysis of the synthesized components showing the existence of Ce, Sm, Zr, and Mg with a total percentage of 100%.

- **Thermogravimetric (TGA) of the synthesized series of $Mg_{x/2}$ doped $Ce_{0.8-x}Sm_{0.2}Zr_{x/2}O_{2-d}$**

Thermogravimetric data was collected on uncalcined samples of $Ce_{0.7}Sm_{0.2}Zr_{0.05}Mg_{0.05}O_{1.9}$ (5%Mg), $Ce_{0.6}Sm_{0.2}Zr_{0.1}Mg_{0.1}O_{1.9}$ (10 %Mg) and $Ce_{0.5}Sm_{0.2}Zr_{0.15}Mg_{0.15}O_{1.9}$ (15%Mg) to know the sintering behavior of the samples. The weight loss started around 60 °C, and lost about 6% until 275 °C which was due to the evaporation of the absorbed water molecule. From 275 °C to 730 °C, another big loss (about 30%) was observed due to the decomposition of some oxides and the organic fuel into different gases, such as nitrogen, carbon dioxide, and water vapors [53]. The final weight loss was observed until 900 °C which was about 15%. Figure 5 illustrates the TGA profile of all 3 samples. There are small differences between the samples which can be neglected. The high-temperature loss is normally related to the chemical reaction [54,55], oxygen vacancy formation, and valence change of the constituting cations. This change confirms the full crystallization and phase formation above 900 °C. All gaseous products generated by volatilization and chemical reaction are transferred from the furnace chamber with the help of N2 gas which guarantees that there is no interference with the sample during thermal treatment. The 50% total weight loss is normal, as we heated the samples under a nitrogen atmosphere to avoid the presence of H_2 or O_2. The high-temperature region of TGA in the nitrogen atmosphere indicates the oxygen loss from the crystallite.

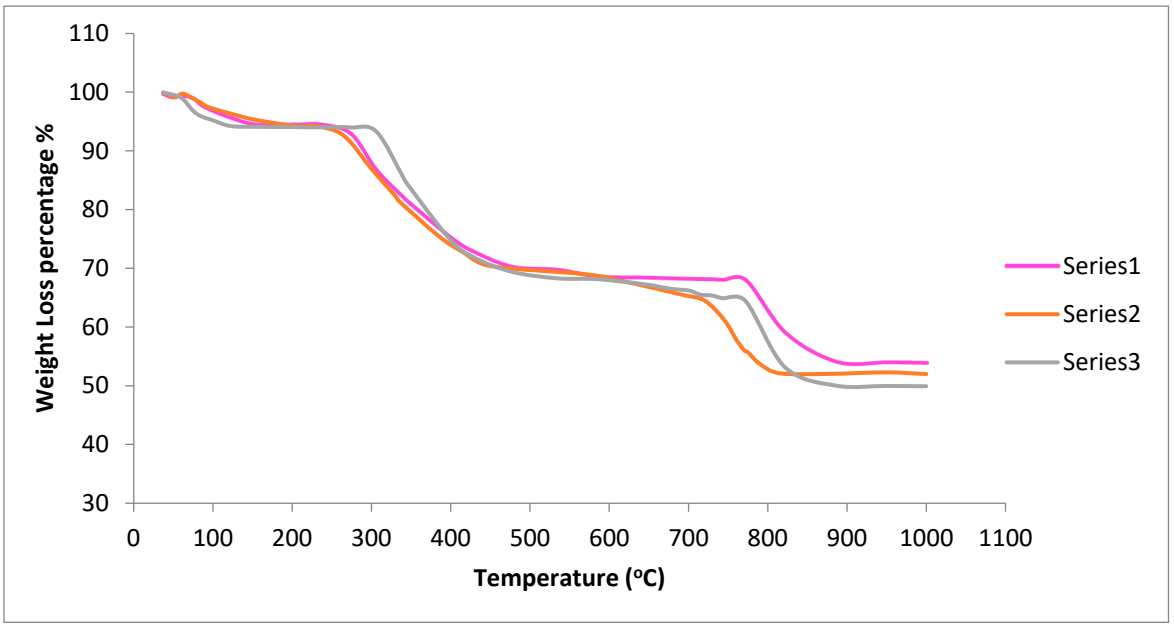

Preprints (www.preprints.org) | NOT PEER-REVIEWED | Posted: 7 June 2023 doi:10.20944/preprints202306.0496.v1

Figure 5. The thermogravimetric plot of CSZM powders for 5% CSZM (Series 1) and 10% CSZM (Series 2) and 15% CSZM (Series 3).

- **Electrochemical Impedance spectroscopy (EIS) of the prepared samples under 5 % H2/Ar.**

The solid electrolyte electrical properties were investigated and studied using (EIS) measurements and based on the given Nyquist plots in the three synthesized compounds total ionic conductivities were evaluated accordingly according to the given data in Table 2, where symmetrical cells testing of the pellets were prepared and EIS measurements were achieved in the wet condition of 5% H_2/Ar.

Table 2. Dimensions of tested pellets during EIS measurements.

Material		Outer diameter	Pt diameter (mm)		Thickness (mm)	Weight without
Code	Compound	(mm)	A	B		Pt (g)
CSZM05	$Ce_{0.7}Sm_{0.2}Zr_{0.05}Mg_{0.05}O_{1.9}$	9.8367	7.0067	7.0500	1.6100	0.4920
CSZM10	$Ce_{0.6}Sm_{0.2}Zr_{0.1}Mg_{0.1}O_{1.9}$	9.6667	6.6367	6.8933	1.5667	0.4855
CSZM15	$Ce_{0.5}Sm_{0.2}Zr_{0.15}Mg_{0.15}O_{1.9}$	9.7267	6.8933	7.0867	1.4900	0.4965

The EIS developed measurements were used in measuring the electrical properties of CSZM compounds and the related electrical properties of the synthesized electrolyte material in a symmetrical cell testing based on anode-supported materials as can be observed from Table 2 and the resultant ionic conductivity was accordingly calculated. Through Nyquist plots and with the fitting results it was easy to identify the needed information about the separate contribution of grain resistance, grain boundary resistance, and electrode process. The EIS measurements were achieved and analyzed using a Solartron 1255 (Schlumberger) frequency response analyzer (0.01 Hz~1 MHz). Results from Nyquist patterns analysis followed the included circuit range of 400 °C to, 700 °C with a step of 50 °C in wet 5% H_2/Ar. Figure 6a,b,c show the fitted impedance plots obtained for CSZM oxides within the range of 400 °C to 700 °C. Resultedin plots were characterized by the start of inductance L1 and followed by semicircles of two regions indicating the polarization resistance Rp from the electrode as grain boundaries [56] along the whole tested ranges

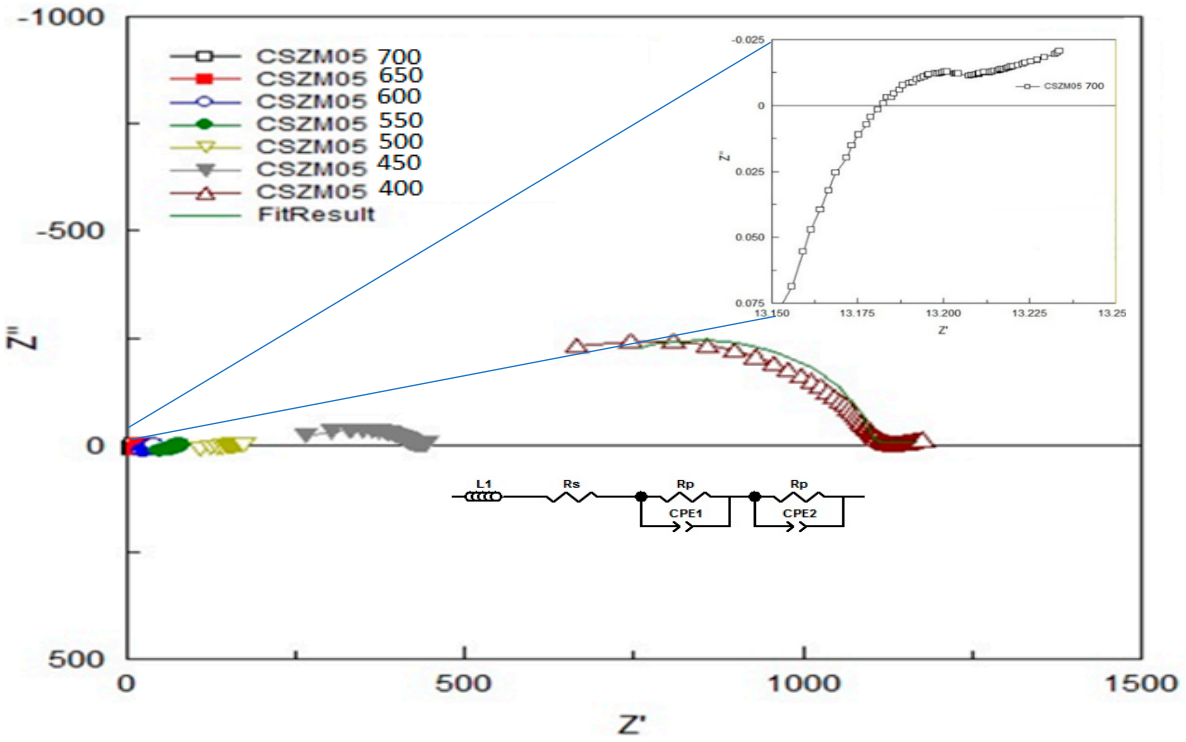

(a)

Preprints (www.preprints.org) | NOT PEER-REVIEWED | Posted: 7 June 2023 doi:10.20944/preprints202306.0496.v1

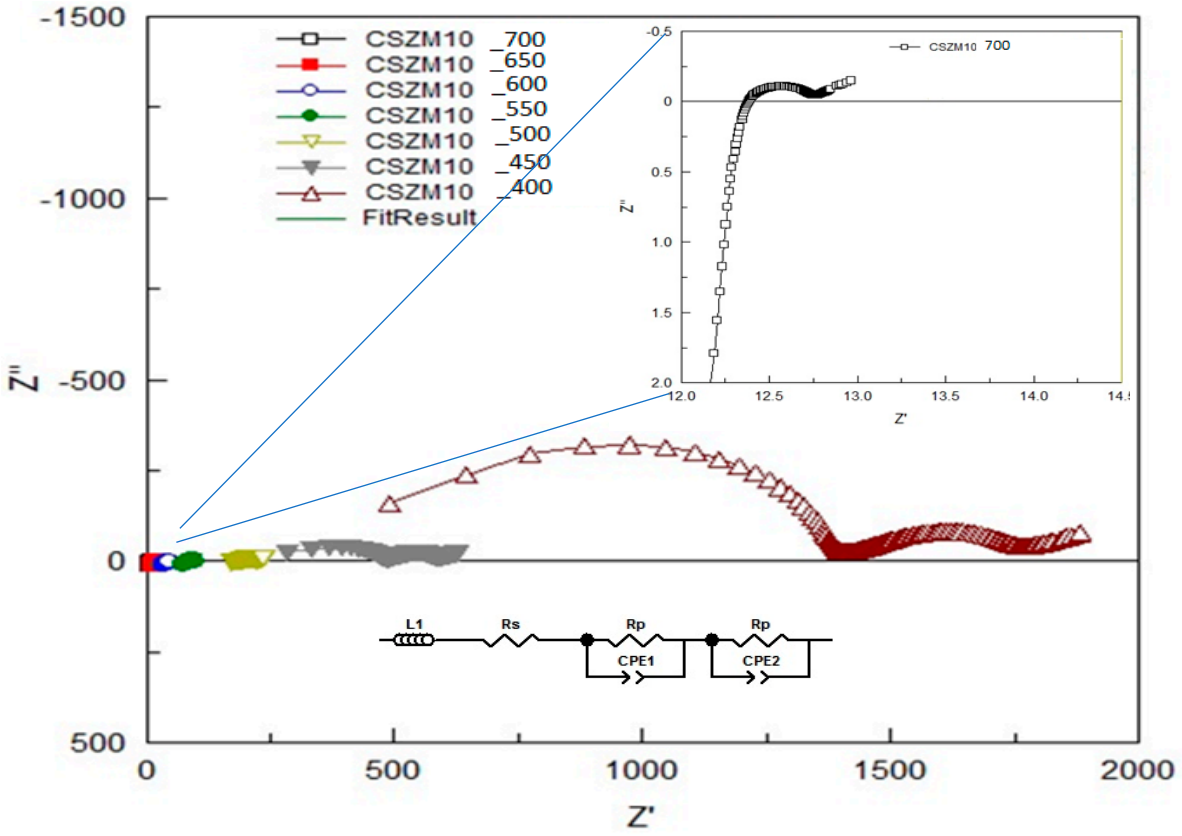

(b)

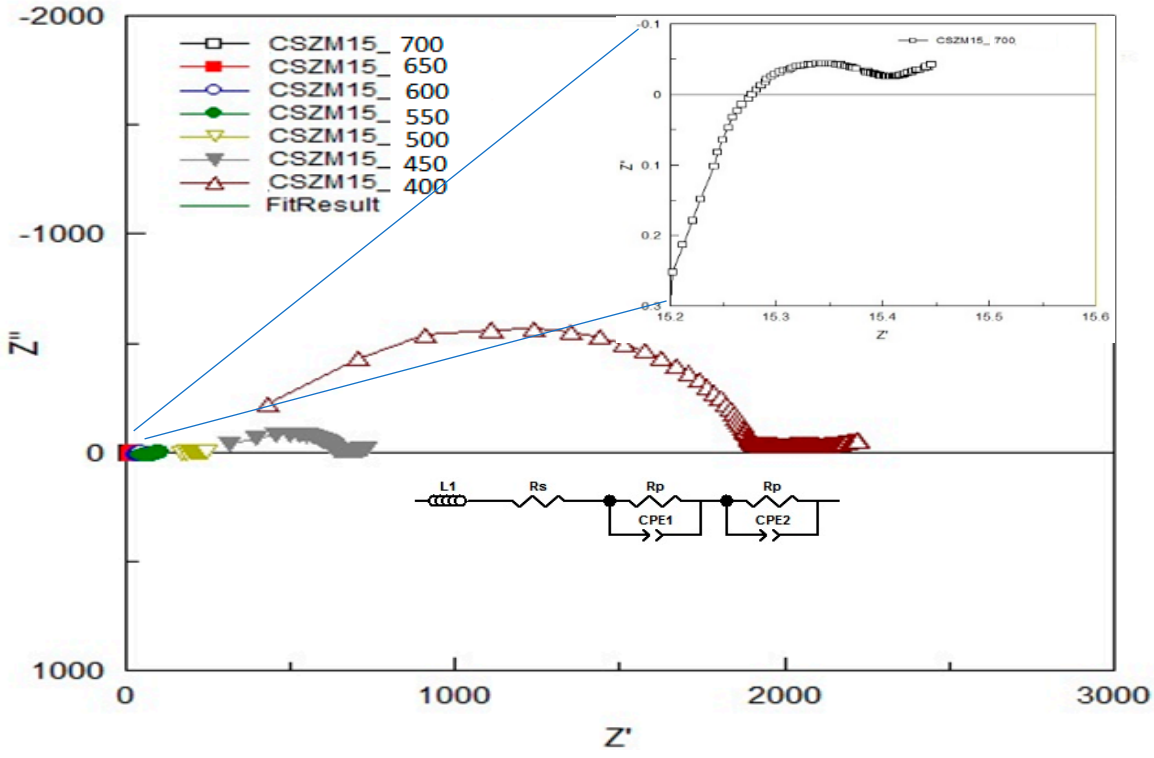

(c)

Figure 6. (a) Fitted EIS plots with equivalent circuits obtained for 5% CSZM oxide within the range of 400 to 700 °C in a 5% H_2 and wet argon atmosphere. **(b)** Fitted EIS plots with equivalent circuits obtained for 10 % CSZM oxides within the range of 400 to 700 °C in a 5% H_2 and wet argon

Preprints (www.preprints.org) | NOT PEER-REVIEWED | Posted: 7 June 2023 doi:10.20944/preprints202306.0496.v1

atmosphere. (**c**) Fitted EIS plots with equivalent circuits obtained for 15 % CSZM oxides within the range of 400 to 700 °C in a 5% H_2 and wet argon atmosphere.

From the analysis and fitting of the EIS plots, the capacitance was calculated for CSZM compounds [56] in a range from 4.45 x 10^{-3} F to 1.16 x 10^{-10} F in a temperature from 400 to 700 °C for 5% doping with a narrow range of polarization resistance values from 3.35 x 10^{-3} Ω to 3.77 x 10^{+1}Ω [49]. For 10% CSZM the values of calculated capacitance were 8.54 x 10^{-3} F to 5.2 x 10^{-11} in the same range of temperature with a range of polarization resistance from 1.55 x 10^{-3} Ω to 1.74 x 10^{+2} Ω. While in the last composition, 15% CSZM the calculated values of capacitance are 8.54 x 10^{-3} F to 5.34 x 10^{-11} with 1.55 x 10^{-2} Ω to 1.34 x 10^{+2}. The total conductivity of the symmetrical cell (σ), the total capacitance (C), and the area-specific resistance (ASR) in addition to the polarization resistance (Ω) values are listed in the following Tables 3–5.

Table 3. The electrical properties values of CSZM of 5 % doping Mg**.**

T (°C)	1/T (K^{-1})	s total (S/cm)	ln (s total) (S/cm)	Ohmic Resistance (Ω)	Capacitance	ASR	Polarization resistance (Ω)
700	0.001027591	1.0461E+01	2.347653318	2.3898E-01	4.45E-03	8.37E-04	3.35E-03
650	0.001083248	3.7979E+00	1.33445878	6.5825E-01	2.32E-04	2.31E-03	9.22E-03
600	0.001145279	6.0300E-01	-0.505841294	4.1460E+00	2.83E-04	1.45E-02	5.81E-02
550	0.001214845	1.3315E-01	-2.016275199	1.8776E+01	6.85E-04	6.58E-02	2.63E-01
500	0.00129341	2.7329E-02	-3.599815363	9.1479E+01	1.73E-03	3.20E-01	1.28E+00
450	0.001382839	5.8143E-03	-5.147432299	4.2997E+02	6.27E-10	1.51E+00	6.03E+00
400	0.001485553	9.2890E-04	-6.981506424	2.6913E+03	1.16E-10	9.43E+00	3.77E+01

Table 4. The electrical properties values of CSZM of 10 % doping Mg.

T (°C)	T (K)	s total (S/cm)	ln (s total) (S/cm)	Ohmic Resistance (Ω)	Capacitance	ASR	Polarization resistance (Ω)
700	0.001027591	2.2639E+00	0.81709542	1.1043E+00	8.54E-03	3.87E-03	1.55E-02
650	0.001083248	4.4590E-01	-0.807654027	5.6066E+00	1.55E-04	1.96E-02	7.86E-02
600	0.001145279	1.6106E-01	-1.825958391	1.5522E+01	6.46E-05	5.44E-02	2.18E-01
550	0.001214845	4.9418E-02	-3.007438747	5.0589E+01	2.49E-05	1.77E-01	7.09E-01
500	0.00129341	7.1712E-03	-4.937684105	3.4862E+02	4.14E-05	1.22E+00	4.89E+00
450	0.001382839	2.3180E-03	-6.067037035	1.0785E+03	5.95E-08	3.78E+00	1.51E+01
400	0.001485553	2.0162E-04	-8.509132304	1.2400E+04	5.20E-11	4.34E+01	1.74E+02

Table 5. The electrical properties values of CSZM of 15 % doping Mg.

T (°C)	T (K)	s total (S/cm)	ln (s total) (S/cm)	Ohmic Resistance (Ω)	Capacitance	ASR	Polarization resistance (Ω)
700	0.001027591	2.2639E+00	0.81709542	1.1043E+00	8.54E-03	3.87E-03	1.55E-02
650	0.001083248	4.4590E-01	-0.807654027	5.6066E+00	1.55E-04	1.96E-02	7.86E-02
600	0.001145279	1.6106E-01	-1.825958391	1.5522E+01	6.46E-05	5.44E-02	2.18E-01
550	0.001214845	4.9418E-02	-3.007438747	5.0589E+01	2.49E-05	1.77E-01	7.09E-01
500	0.00129341	1.1081E-02	-4.502482338	2.2560E+02	1.01E-05	7.90E-01	3.16E+00
450	0.001382839	1.5281E-03	-6.483742838	1.6360E+03	1.07E-06	5.73E+00	2.29E+01
400	0.001485553	2.6192E-04	-8.247487205	9.5450E+03	5.34E-11	3.34E+01	1.34E+02

It was clear from the given results listed in the above tables that the compounds of CSZM electrolyte materials are showing remarkable values in the measured conductivities however there is a small gap in the total conductivities between the 5% CSZM and 15% CSZM but they are still higher than some reported electrolyte materials [57]. The Arrhenius plots in Figure 7 demonstrated that $Ce_{0.7}Sm_{0.2}Zr_{0.05}$ $Mg_{0.05}O_{1.9}$ is showing ahigher value of 1.0461 x 10^{+1} S/cm at 700 °C while the minimum value was 2.7329 x 10^{-2} S/cm at 400 °C and the total activation energy was found E_a 0.6865 eV. The CSZM 5% was the highest in conductivity values compared to both 10% and 15% CSZM and that returns to the highly dense electrolyte materials as some pores occurred in them. This was noticed

Preprints (www.preprints.org) | NOT PEER-REVIEWED | Posted: 7 June 2023 doi:10.20944/preprints202306.0496.v1

from the SEM images. Meanwhile, the occurrence of this porosity still gives higher values of conductivities compared to the previously investigated electrolyte materials [58] and this can be observed from plotted Arrhenius plots in Figure 7 under 5% H_2/Argon wet atmosphere.

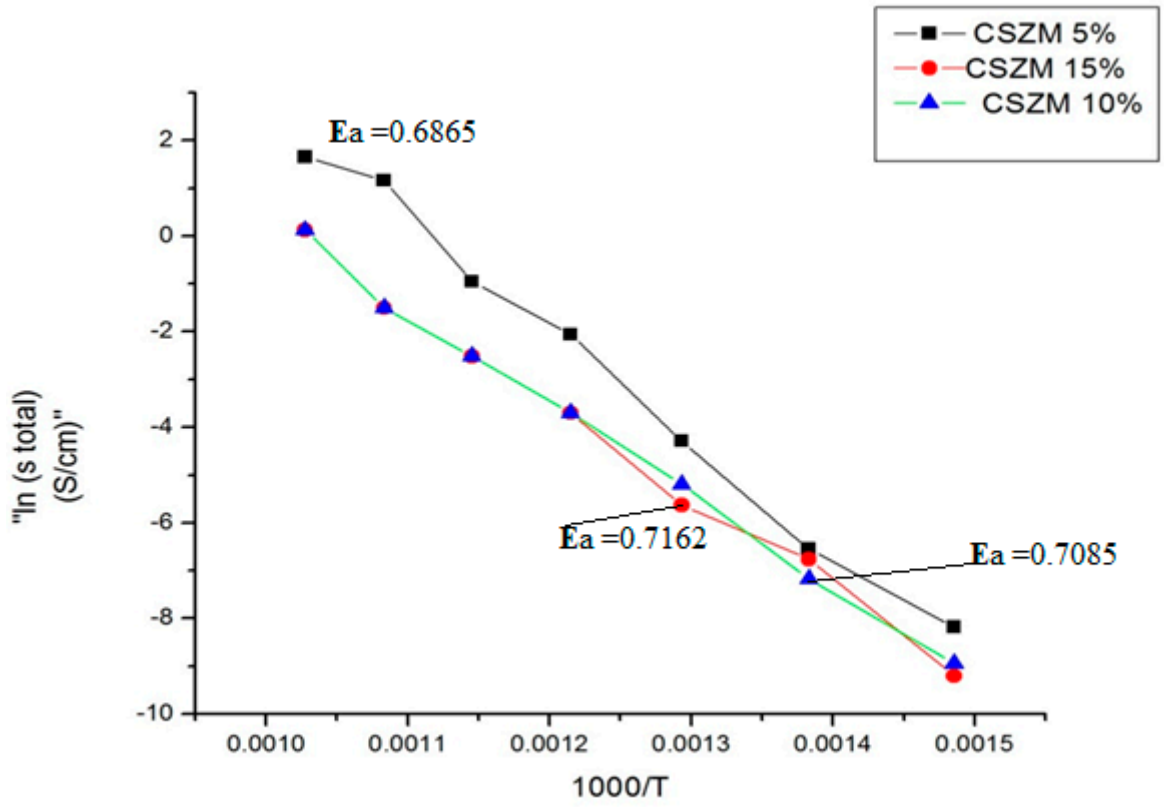

Figure 7. Arrhenius plots of CSZM conductivity 5%, 10%, and 15% under 5%H_2/Argon.

The CSZM electrolyte conductivity at 700 °C with 5% dopant has shown a higher value and it was higher than the reported ones in multi-dopant ceria electrolytes [59–62] and this because of the ordering of oxygen vacancies with small ionic radii and mobility makes these materials very conductive. However, the other 10% and 15% showed lower values due to the occurrence of voids and pores which can be overcome with doping of some materials in B sight like lithium oxide, [63] or Zin oxides [64] and it can be achieved at lower range of temperature and less than 1400 °C. The most essential finding of Mg doping for giving the higher conductivity values other than porosity and density in all synthesized series is due to the Mg doping altered the electronic structure [65] of the host compound by altering the ion bond and crystal layer gap, and the chemical bond length between the doped and O atoms is proportional to the atomic radius of the doped cations.

4. Conclusion and Recommendations

Due to the investigated materials with different percentage dopants of Mg and Zr with 5, 10, and 15% in the CSZM electrolyte materials compounds. The obtained results showed remarkable findings when the compounds were characterized physically and electrochemically with higher stability and conductivity in symmetrical cell testing. Structural analyses of the synthesized compounds were achieved accurately after careful analysis and refinement, showing the materials crystallized in a pure phase fluorite cubic structure with the goodness of the fitting in the (S.G. Fm3m) with a cell parameter value of 5.401742 $°A$ after the final sintering temperature of 1400°C. Highly dense materials appeared in the SEM images, especially in 5% dopant and some pores existed in both 10 and 15%. However, there were some pores in the 10 and 15% dopant but still showed higher values in conductivities compared to similar materials reported before. EIS analysis indicates that the 5%

CSZM under investigation of 5% H_2/Ar atmosphere shower highest value of conductivity 2.347 S/cm at 700 °C higher than the previously similar reported electrolyte materials. The doping of 5% Mg showed higher conductivity a bit higher than investigated compounds from literature when comparing it with the microstructure features in terms of densification and porosity. It can be observed clearly from SEM images that 5% have higher densification over the other two percentages that in 10 and 15 % give higher porosity. This important notice can increase more densification with an increase of oxide-ion conductivity by adding zinc oxide or lanthanum oxides with an expectation of higher performance and less sintering temperature.

Author Contributions: Conceptualization, A. M. A; formal analysis, A. M. A and M.K.D; writing—original draft and final paper preparation A. M. A; writing—review and editing, M.K.D J.T and A.K.A.; supervision J.T and A.K.A; project administration, J.T ; funding acquisition, J.T. All authors have read and agreed to the published version of the manuscript.

Funding: This research was financially supported by Prince of Songkla University and the Ministry of Higher Education, Science, Research and Innovation under the Reinventing University Project (Grant Number REV65012).

Institutional Review Board Statement: Not applicable.

Informed Consent Statement: Not applicable.

Data Availability Statement: Not applicable.

Acknowledgments: All authors are highly acknowledged by the scientific equipment center (PSU) for supporting this work.

Conflicts of Interest: There is no conflict of interest.

References

[1] Wolfram T, Ellialtioglu S, Electronic and Optical Properties of d-Band Perovs, in*: Univ. Press. Cambridge, **2006***.

[2] Tejuca L.G, Fierro J.L.G, Tascón J.M.D, Structure and Reactivity of Perovskite-Type Oxides, *Adv. Catal. **1989***.

[3] Hossain S, Abdalla AM, Jamain SNB, Zaini JH, Azad AK. A review on proton conducting electrolytes for clean energy and intermediate temperature-solid oxide fuel cells. *Renew Sustain Energy Rev **2017**,79,750–64.*

[4] Levy M.R, Chapter 3: Perovskite Perfect Lattice, in: Cryst. Struct. Defect Prop. Predict. *Ceram. Mater., **2005***.

[5] Johnsson M, Lemmens P, Crystallography and Chemistry of Perovskites, in: Handb. Magn. *Adv. Magn. Mater., **2007***.

[6] Taimoor Raza , Jingjing Yang , Ruoming Wang , Chen Xia ,Rizwan Raza , Bin Zhu , Sining Yun "Recent advance in physical description and material development for single component SOFC: A mini-review" Chemical Engineering Journal, Volume 444, 15 September 2022, 136533.

[7] Muneeb Irshad,Naila Kousar,Muhammad Bilal Hanif, Asif Nadeem Tabish, Abdul Ghaffar, Muhammad Rafique, Khurram Siraj, Zeeshan Aslam,Mohammed A. Assiri, Muhammad Imran, Michał Mosiałek, Zuzana Zmrhalovahi and Martin Motola "Investigating the microstructural and electrochemical performance of novel La0.3Ba0.7Zr0.5X0.3Y0.2 (X = Gd, Mn, Ce) electrolytes at intermediate temperature SOFCs.Sustainable Energy Fuels, 2022,6, 5384-5391

[8] Zia UdDin, Z.A.Zainal, Biomass integrated gasification–SOFC systems: Technology overview, *Renewable and Sustainable Energy Reviews, **2016**, 53,1356–1376.*

[9] Radenahmad, N., Azad, A.T., Saghir, M., Taweekun, J., Bakar, M.S.A., Reza, M.S., Azad, A.K., "A review on biomass derived syngas for SOFC based combined heat and power application", *Renewable and Sustainable Energy Reviews*, 2020, 119, 109560.

[10] Giovanni Capurso et al., Nanoconfined mixed Li and Mg borohydrides as materials for solid state hydrogen storage, *Int. J. Hydrogen Energy **2012**, 37, 14, 10768-10773*

[11] N. Radenahmad, J. Taweekun, A. Afif, J. I. Lee, J.-Y. Park, J. Zaini, A. K. Azad, "Syngas Fuelled High Performance Solid Oxide Fuel Cell", *ECS Transactions*, 2019, 91(1), 1621-1629.

[12] P.V. Aravind, T.Woudstra, N.Woudstra, H. Spliethoff, Thermodynamic evaluation of small-scale systems with biomass gasifiers, solid oxide fuel cells with Ni/GDC anodes and gas turbines , *Journal of Power Sources* ***2009***,*190, 461–475*

[13] Pukazhselvan D, K Sandhya, Nasani N, Paul D. Chemical transformation of additive phase in MgH_2/CeO_2 hydrogen storage system and its effect on catalytic performance. *Appl Surf Sci* ***2021***,*561,150062.*

[14] Q. Zhang, W.J. Liu, J. Wang, D. Liu, Z.H.C. Sun, Processing of perovskite $La_{0.9}Sr_{0.1}Ga_{0.8}Mg_{0.2}O_{3-\delta}$ electrolyte by glycine-nitrate combustion method, *Int. J. Hydrogen Energy* ***2021***,*46,61, 31362-31369.*

[15] Nagar R, Vinayan B, Samantaray P, Ramaprabhu S. Recent advances in hydrogen storage using catalytically and chemically modified graphene nanocomposites. *J Mater Chem A* ***2017***;*5(44):22897-912.*

[16] Peng D, Ding Z, Fu Y, Wang Y, Bi J, Li Y, Han S. Enhanced H2 sorption performance of magnesium hydride with hard-carbon-sphere-wrapped nickel. *RSC Adv* ***2018***;*8(50): 28787-96.*

[17] Zhang X, Liu Y, Zhang X, Hu J, Gao M, Pan H. Empowering hydrogen storage performance of MgH_2 by nanoengineering and nanocatalysis. *Mater Today Nano* ***2020***,*9,100064.*

[18] Ma Z, Zhang Q, Zhu W, Khan D, Hu C, Huang T, Ding W, Zou J. Nano Fe and Mg2Ni derived from TMA-TM (TM=Fe, Ni) MOFs as synergetic catalysts for hydrogen storage in MgH2. *Sustain Energ Fuels* ***2020***;*4(5):2192-200.*

[19] Abdalla A, Hossain S, Nisfindy O, Azad A, Dawood M, Azad A. Hydrogen production, storage, transportation and key challenges with applications: A review. *Energ Convers Manage* ***2018***,*165,602-27.*

[20] Mohtadi R, Orimo S. The renaissance of hydrides as energy materials. *Nat Rev Mater* ***2016***;*2(3):16091.*

[21] Serge Nyallang Nyamsi et al., 200 NL H_2 hydrogen storage tank using MgH_2eTiH_2eC nanocomposite as H_2 storage Material, *Int.J. Hydrogen Energy*,***2021***, *46 ,36, 19046-19059.*

[22] Ouyang L, Chen K, Jiang J, Yang X, Zhu M. Hydrogen storage in light-metal based systems: A review. *J Alloys Compd* ***2020***,*829,154597.*

[23] Huang Z, Guo Z, Calka A, Wexler D, Lukey C, Liu H. Effects of iron oxide (Fe_2O_3, Fe_3O_4) on hydrogen storage properties of Mg-based composites. J Alloys Compd **2006**;422,1-2,299-304.

[24] Zhang X, Wang K, Zhang X, Hu J, Gao M, Pan H, Liu Y. Synthesis process and catalytic activity of Nb_2O_5 hollow spheres for reversible hydrogen storage of MgH_2. *Int J Energ Res* ***2020***;*45,2,3129-41.*

[25] Shahi R, Tiwari A, Shaz M, Srivastava O. Studies on de/rehydrogenation characteristics of nanocrystalline MgH2 co-catalyzed with Ti, Fe and Ni. *Int J Hydrogen Energy* ***2013***;*38,6,2778-84.*

[26] Shevlin S, Guo Z. MgH2 Dehydrogenation Thermodynamics: Nanostructuring and Transition Metal Doping. *J Phys Chem C* ***2013***;*117,21,10883-91.*

[27] Ponthieu M, Calizzi M, Pasquini L, Fernández J, Cuevas F. Synthesis by reactive ball milling and cycling properties of MgH2-TiH2 nanocomposites: Kinetics and isotopic effects. *Int J Hydrogen Energy* ***2014***;*39,18,9918-23.*

[28]Souza ECC De, Muccillo R. Properties and applications of perovskite proton conductors. *Mater Res* ***2010***,*13,385–94.*

[29]Haugsrud R, Norby T. Proton conduction in rare-earth ortho-niobates and ortho-tantalates. *Nat Mater* ***2006***,*5,193–6.*

[30]Fabbri E, Pergolesi D, Traversa E. Materials challenges toward proton conducting oxide fuel cells: a critical review. Chem *Soc Rev* ***2010***,*39,4355–69.*

[31]Duan C, Tong J, Shang M, Nikodemski S, Sanders M, Ricote S, et al. Readily processed protonic ceramic fuel cells with high performance at low temperatures. *Sci Rep* ***2015***,*349,1321–6.*

[32] Kreuer KD. Proton-Conducting Oxides. *Annu Rev Mater Res* ***2003***,*33,333–59.*

[33] Muneeb Irshad, Mehak Khalid, Muhammad Rafique, Naveed Ahmad, Khurram Siraj, Rizwan Raza, Muhammad Sadiq, Muhammad Ahsan, Abdul Ghaffarg and Amina Ashfaq "Evaluation of BaCo0.4Fe0.4Zr0.2−xNixO3−δ perovskite cathode using nickel as a sintering aid for IT-SOFC,RSC Adv., 2021,11, 14475-14483.

[34] Wei Zhang, Yun Hang Hu "Recent progress in design and fabrication of SOFC cathodes for efficient catalytic oxygen reduction Author links open overlay panel" Catalysis Today Volume 409, 1 February 2023, Pages 71-86.

[35] Fabbri E, Pergolesi D, Traversa E. Electrode materials: A challenge for the exploitation of protonic solid oxide fuel cells. Sci *Technol Adv Mater* ***2010***,*11,044301.*

[36]Bonano N, Ellis B, Mahmood MN. Construction and operation of fuel cells based on the solid electrolyte $BaCeO_3$,Gd. *Solid State Ionics* ***1991***;*44,305-11.*

[37]Ma GL, Shimura T, Iwahara H. Ionic conduction and nonstoichiometry in $Ba_xCe_{0.90}Y_{0.10}O_{3-\delta}$. *Solid State Ionics* ***1998***,*110,103–10.*

[38]Schober T, Bohn HG. Water vapor solubility and electrochemical characterization of the high temperature proton conductor $BaZr_{0.9}Y_{0.1}O_{2.95}$. *Solid State Ionics* ***2000***,*127,351-60*.

[39]Kreuer KD, Adams S, Münch W, Fuchs A, Klock U, Maier J. Proton conducting alkaline earth zirconates and titanates for high drain electrochemical applications. *Solid State Ionics*, ***2001***;*145,295-306*.

[40] V.A. Yartys et al., Magnesium based materials for hydrogen based energy storage: Past, present and future, *Int. J. Hydrogen Energy* ***2019***,*44, 15, 7809-7859.*

[41] Jianjiang Hu, Maximilian Fichtner, Marcello Baricco Preparation of Li-Mg-N-H hydrogen storage materials for an auxiliary power unit , *Int.J. Hydrogen Energy* ***2017***, *42, 27, 17144-17148.*

[42] Jingfeng Xue, Yu Shen, Qingjun Zhou, Tianmin He, Yanhong Han Combustion synthesis and properties of highly phase-pure perovskite electrolyte Co-doped $La_{0.9}Sr_{0.1}Ga_{0.8}Mg_{0.2}O_{2.85}$ for IT-SOFCs *Int. J. Hydrogen Energy****2010****, 35,1, 294-300.*

[43] Jos_e Juan Alvarado Flores et al., Advances in the knowledge of the double perovskites derived from the conformation and substitution of the material Sr_2MgMoO_{6-d} as anode with potential application in SOFC cell, *Int. J. Hydrogen Energy* ***2021***,*46,51, 26152-26162.*

[44] Daniel Friedrich, Marc Schlosser, and Arno Pfitzner. Synthesis, Crystal Structure, and Physical Properties of Two Polymorphs of $CsGaSe_2$, and High-Temperature X-ray Diffraction Study of the Phase Transition Kinetics. *J Cryst. Growth Des.* ***2016***,*16 3983−399.*

[45] Lufaso MW, Woodward PM. research papers Prediction of the crystal structures of perovskites using the software program *J. Acta Crystallography B,* ***2001***,*725–38.*

[46] Mustafa Anwar, Muhammed Ali S.A, Abdalla M. Abdalla, Mahendra Rao Somalu, Andanastuti Muchtar, Effect of sintering temperature on the microstructure and ionic conductivity of $Ce_{0.8}Sm_{0.1}Ba_{0.1}O_{2-d}$ electrolyte, *Processing and Application of Ceramics* ***2017***,*11,1,67–74.*

[47] Muneeb Irshad , Raazia Idrees, Khurram Siraj, Imran Shakir , Muhammad Rafique , Qurat ul Ain , Rizwan Raza

"Electrochemical evaluation of mixed ionic electronic perovskite cathode LaNi1-xCoxO3-δ for IT-SOFC synthesized by high temperature decomposition Author links open overlay panel. International Journal of Hydrogen Energy, Volume 46, Issue 17, 8 March 2021, Pages 10448-10456.

[48] Risheng Pei, Sandra Korte-Kerzel, Talal Al-Samman "Normal and abnormal grain growth in magnesium: Experimental observations and simulations" Journal of Materials Science & Technology, Volume 50, 1 August 2020, Pages 257-270.

[49] W.D. Kingery, H.K. Bowen, D.R. Uhlmann, Introduction to Ceramics, *John Wiley & Sons, New York,* ***1976***.

[50] M.N. Rahaman, Ceramic Processing and Sintering, *Marcel Dekker Inc., New York,* ***1995***.

[51] L. Chen, D.F. Zhou, Y. Wang, X.F. Zhu, J. Meng, "Enhanced sintering of $Ce_{0.8}Nd_{0.2}O_2$, $La_{0.8}Sr_{0.2}Ga_{0.8}Mg_{0.2}O_3$, using CoO as a sintering aid*", Ceram. Int.,* ***2017***,*43,4,3583–3589.*

[52] J. Xiong, C. Jiao, M. Han, W. Yi, J. Ma, C. Yan, W. Cai, H. Cheng, "Effect of Li2O additions upon the crystal structure, sinterability and electrical properties of yttria stabilized zirconia electrolyte", *RSC Adv.****2016****,6, 106555–106562.*

[53] Cun Xin Guo, Jian Xin Wang, Chang Rong He, Wei Guo Wang, Effect of alumina on the properties of ceria and scandia co-doped zirconia for electrolyte-supported SOFC, *Ceram.In,* ***2013****, 39,8, 9575-9582.*

[54] S. Gill, R. Kannan, N. Maffei V.Thangadurai "Effect of Zr substitution for Ce in BaCe0.8Gd0.15Pr0.05O3−δ on the chemical stability in CO2 and water, and electrical conductivity" RSC Adv., 2013,3, 3599-3605

[55] Kannan, R., Singh, K., Gill, S. et al. Chemically Stable Proton Conducting Doped BaCeO3 -No More Fear to SOFC Wastes. Sci Rep 3, 2138 (2013). https://doi.org/10.1038/srep02138

[56]E. Barsoukov and J. R. Macdonald, Impedance Spectroscopy: Theory, Experiment, and Applications. *John Wiley & Sons, Inc.,* ***2005***.

[57] D. Chen, R. Ran, K. Zhang, J. Wang, and Z. Shao. Intermediate-temperature electrochemical performance of a polycrystalline $PrBaCo_2O_{5+\delta}$ cathode on samarium-doped ceria electrolyte. *J. Power Sources.* ***2009,****188,1 96–105.*

[58] Bin Lin, Songlin Wang, Xingqin Liu, Guangyao Meng, Simple solid oxide fuel cells*, J. A.& Compounds,* ***2010****,490, 1–2, 214-222.*

[59] Riccardo Polini, Arianna Pamio, Enrico Traversa, Effect of synthetic route on sintering behaviour, phase purity and conductivity of Sr- and Mg-doped LaGaO3 perovskites, *J. E. Ceramic Society* ***2004***, *24,6, 1365-1370.*

[60] J. Yang, B. Ji, J. Si, Q. Zhang, Q. Yin, J. Xie, C. Tian, Synthesis and properties of ceria based electrolyte for ITSOFCs*", Int. J. Hydrogen Energy*, ***2016,****41,36,15979– 15984.*

[61] X. Sha, Z. Lü, X. Huang, J.Miao, Z. Liu, X. Xin, Y. Zhang, W. Su, "Influence of the sintering temperature on electrical property of the Ce0.8Sm0.1Y0.1O1.9 electrolyte", *J. Alloys Compd.*, ***2007****,433,1-2, 274–278.*

[62] S.J. Hong, A.V. Virkar, "Lattice parameters and densities of rare-earth oxide doped ceria electrolytes", *J. Am. Ceram. Soc.*, ***1995****,78,2, 433–439.*

[63] M. Kahlaoui, S. Chefi, A. Inoubli, A. Madani, C. Chefi, Synthesis and electrical properties of co-doping with La^{3+}, Nd^{3+}, Y3+, and Eu3+ citric acid-nitrate prepared samarium-doped ceria ceramics", *Ceram. Int* ***2013****, 39,4, 3873–3879*.

[64] Jin Peng, Shuang Zhao, Asif Hassan Raza, Yan Wu. Energy band modulation of Mg-doped ZnO electrolyte for low-temperature advanced fuel cells" *Int. J. of Hydrogen Energy* ***2023****, 48, 15, 6088-6098.*

[65] Mahmood Hameed Majeed , Murat Aycibin , Arife Gencer Imer"Study of the electronic, structure and electrical properties of Mg and Y single doped and Mg/Y co-doped ZnO: Experimental and theoretical studies" Optik,Volume 258, May 2022, 168949